A Graphical Solution of the Direct Kinematic Problem of Star Translational Parallel Manipulators

Mamdouh SAYD, Luc BARON and Christian MASCLE
Department of Mechanical Engineering
École Polytechnique de Montréal
P.O. 6079, station Centre-Ville
Montréal, Québec, Canada, H3C 3A7
mamdouh.sayd@polymtl.ca, luc.baron@polymtl.ca, christian.mascle@polymtl.ca

Abstract

This paper presents a graphical solution method to solve the direct kinematic problem of Star translational parallel manipulators of general geometry. The method allows to find all real solutions of this problem from a given set of actuated joint positions, which is equivalent to find the intersection points of three meridian-circular screw surfaces. Algebraically, this problem reduces to solve six nonlinear equations in six unknowns, from which it may exist more than two reals solutions.

Résumé

Cette article présente une méthode de solution graphique du probleme géométrique direct des manipulateurs translationels Star de géométrie générale. Cette méthode permet le calcul de toutes les solutions réelles de ce probleme pour des positions connues des actionneurs, qui est équivalente á déterminer les points d'intersections de trois surfaces hélicoidale á méridien circulaire. Algébriquement, ce probleme réduit á la solution de six équations nonlinéaires á six inconnus pour lequel il peut exister plus de two solutions réels.

1 Introduction

Robotic manipulators can be classified in four different categories, i.e., serial, parallel, tree-type and hybrid, based on the structure of their chain. In general, parallel manipulators (PMs) consist of two main bodies coupled via n legs. The fixed body is designed as the base, while the other is movable and called the end-effector (EE) of the manipulator. As shown in Fig.1, the Y Star PM [1] is capable to generate 3D translations of its EE, at constant orientation, and hence, is designated as a translational parallel manipulator (TPM). The direct kinematic (DK) problem pertains to determine the EE pose—i.e. the position and the orientation—from a set of joint positions. Conversely, the inverse kinematic problem (IK) consists to determine the actuated joint positions from the pose of the EE. For PM, the latter is usually straightforward, while the former is much more

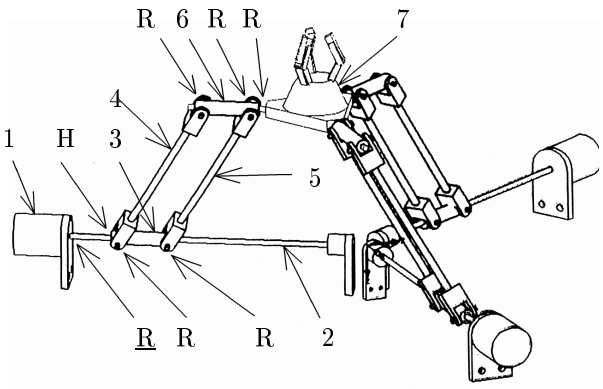

Figure 1: The Y Star TPM of topology 3-RHΠR

challenging [2]. The different DK solutions are also called assembly modes, since they correspond to different ways of assembling the PM, for a given set of actuated joint positions.

For the Star TPM, it is possible to assemble each leg to the EE above and below the plan of the three screws, while maintaining the position of link 3 along the three screw axes, and hence, the Star should have only two assembly modes. Although this reasoning being perfectly true, the Star TPM doesn't maintain the position of link 3, but rather maintains the rotation of link 2 with the three motorized revolute joints. Thus, a rotation of the 4-bar linkage around its corresponding screw produces a passive displacement of link 3 along the screw axis based on the pitch of the screw. Several authors (e.g.,[3]) have neglected this passive displacement, including the authors themselves of this paper [4, 5]. This paper presents a graphical solution of the DK problem of Star TPMs of general geometry and shows that these TPMs can have more than two real assembly modes.

2 Kinematic Model

The kinematics of robotic manipulators can be described with the concept of *kinematic chain*, which carries both topological and geometrical informations. A kinematic chain is defined as a mechanical system in which rigid bodies, called *links*, are coupled by *lower kinematic pairs*. There are six of such pairs, namely, revolute (R), prismatic (P), cylindrical (C), helicoidal (H), planar (E), and spherical (S). Moreover, a circular path at constant orientation describes by the output link of planar 4-bar RRRR linkages is assimilated as a 1-DOF pair, namely the Π joint [6]. The *topology* refers to the layout of these pairs along the chain, while the *geometry* refers to the relative location of the pairs on each link. The Star TPM is composed of three chains of topology RHΠR, i.e., an actuated R joint—denoted R—connecting link 1 to link 2 (also called the screw), a passive H joint connecting link 2 to 3, two passive R joints connecting links 4 and 5 (also called the leg) to link 6, and a passive R joint connecting link 6 to link 7, i.e., the EE.

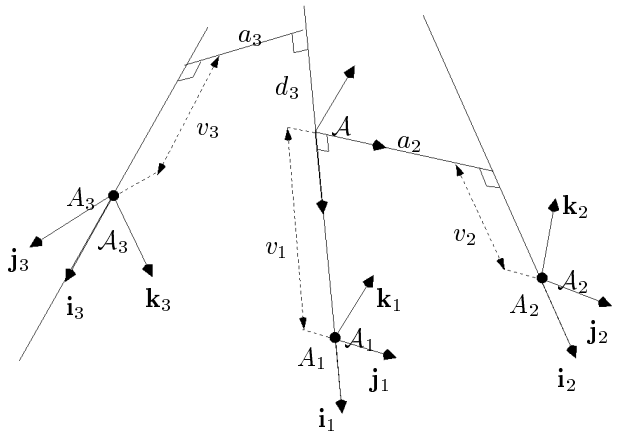

Figure 2: Geometric parameters of the base

2.1 Geometric Parameters

The general geometry of the base A can be described in frame $\mathcal{A}$ with three frames $\{\mathcal{A}_i\}_1^3$ located at points $\{A_i\}_1^3$ with there respective x-axis along the actuated screw axis $\{\mathbf{e}_i\}_1^3$. As shown in Fig. 2, the position vectors of points A_i are given in $\mathcal{A}$ as

$$\begin{aligned} \mathbf{a}_1 &= v_1\mathbf{i}, \quad \mathbf{a}_2 = a_2\mathbf{j} + \mathbf{R}_y(\alpha_2)v_2\mathbf{i}, \\ \mathbf{a}_3 &= d_3\mathbf{i} + \mathbf{R}_x(\beta_3)(a_3\mathbf{j} + \mathbf{R}_y(\alpha_3)v_3\mathbf{i}), \end{aligned} \tag{1}$$

while the orientation of the actuated screw axes are given in $\mathcal{A}$ as

$$\mathbf{e}_i = \mathbf{R}_i\mathbf{i}, \quad i = 1, 2, 3, \tag{2}$$

with $\mathbf{R}_i$ defined as the orientation of $\mathcal{A}_i$ in $\mathcal{A}$, i.e.,

$$\mathbf{R}_1 \equiv \mathbf{1}, \ \mathbf{R}_2 \equiv \mathbf{R}_y(\alpha_2), \ \mathbf{R}_3 \equiv \mathbf{R}_x(\beta_3)\mathbf{R}_y(\alpha_3), \tag{3}$$

where v_1, a_2, α_2, v_2, d_3, β_3, a_3, α_3 and v_3 are the nine geometric parameters allowing to describe the general geometry of the base, $\mathbf{R}_a(\beta)$ denotes the 3×3 rotation matrix of an angle β around axis a, while $\mathbf{i}$, $\mathbf{j}$, $\mathbf{k}$ are the unit vectors along x-, y- and z-axis, respectively. In order to maintain the translational mobility of the EE, the passive revolute joint axes between links 2-3 and 6-7 must always be parallel to the actuated joint axis $\mathbf{e}_i$ of the corresponding leg. Therefore, the rotation matrix describing in $\mathcal{A}$ the orientation of frame $\mathcal{B}$ attached to the EE, denoted B, is given as

$$\mathbf{R}_{\mathcal{B}}^{\mathcal{A}} = \mathbf{1}_{3\times 3}. \tag{4}$$

In this context, the geometry of the EE can be described with the help of three arbitrarily located points $\{B_i\}_1^3$ together with the same unit vectors $\{\mathbf{e}_i\}_1^3$ along the passive revolute joint axes connecting links 6 to the EE. The

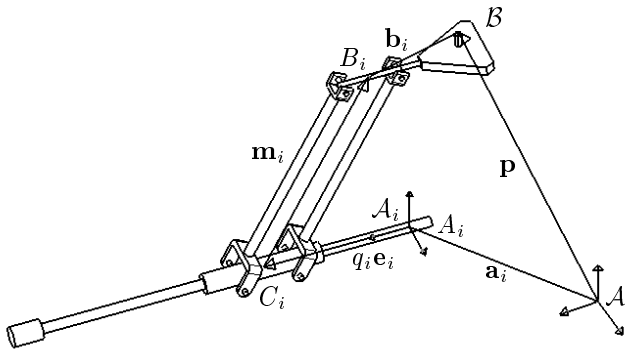

Figure 3: Kinematic loop of leg i

position vectors of points B_i in frame $\mathcal{B}$ are given as

$$\mathbf{b}_1 = v_1'\mathbf{i}, \quad \mathbf{b}_2 = a_2'\mathbf{j} + \mathbf{R}_y(\alpha_2)v_2'\mathbf{i},$$
$$\mathbf{b}_3 = d_3'\mathbf{i} + \mathbf{R}_x(\beta_3)(a_3'\mathbf{j} + \mathbf{R}_y(\alpha_3)v_3'\mathbf{i}) \tag{5}$$

where v_1', a_2', v_2', d_3', a_3' and v_3' are the six geometric parameters describing the geometry of the EE.

2.2 Closure Equation

Each leg of the parallel manipulator defines a kinematic loop passing through the origin of frames $\mathcal{A}$ and $\mathcal{B}$, and points A_i, C_i and B_i. As shown in Fig. 3, the closure of each kinematic loop can be expressed in the form

$$\mathbf{a}_i + q_i\mathbf{e}_i + \mathbf{m}_i = \mathbf{p} + \mathbf{b}_i, \quad i = 1, 2, 3 \tag{6}$$

where q_i is the displacement of C_i relative to A_i along the screw axis $\mathbf{e}_i$, $\mathbf{m}_i$ the position vector B_i relative to C_i in $\mathcal{A}$, and finally, $\mathbf{p}$ the position vector of the origin of $\mathcal{B}$ in $\mathcal{A}$. The knowledge of the actuated joint angle θ_i doesn't allow directly to compute q_i, the corresponding displacement of C_i from A_i along $\mathbf{e}_i$. Indeed, q_i is composed of two displacements: an actuated displacement q_{ia} due to the rotation θ_i of the motor, and a passive displacement q_{ip} due to the rotation γ_i of the leg around the screw axis, and hence, we have

$$q_i = q_{a\,i} + q_{pi} = \frac{p_i}{2\pi}(\theta_i + \gamma_i) \tag{7}$$

where p_i is the pitch of screw i. As shown in Fig.4, vector $\mathbf{m}_i$ depends on γ_i, but also on the other passive (and unknown) rotation ϕ_i around the Π joint of the 4-bar linkage, which can be written as

$$\mathbf{m}_i = l_i\mathbf{R}_i\mathbf{R}_x(\gamma_i)\mathbf{R}_y(\phi_i)\mathbf{k}. \tag{8}$$

The unknown γ_i greatly complicates the kinematics of this manipulator, since it appears linearly in eq.(7) and through transcendental functions in eq.(8).

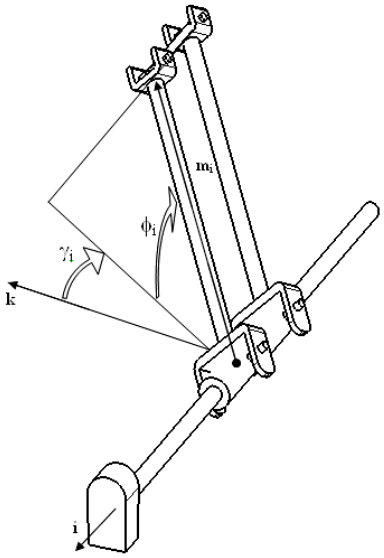

Figure 4: Vector $\mathbf{m}_i$ depends on both γ_i and ϕ_i angles

2.3 Inverse Kinematic Problem

For a given manipulator geometry, the IK is to find the actuated joint positions $\{\theta_i\}_1^3$ from a known position $\mathbf{p}$ of the EE. Since the length of each leg—link 4 in Fig.1—is l_i, computing the norm of $\mathbf{m}_i$ with eq.(6) gives

$$q_i^2 - 2q_i\mathbf{e}_i^T\mathbf{u}_i + \mathbf{u}_i^T\mathbf{u}_i - l_i^2 = 0, \tag{9}$$

with $\mathbf{u}_i$ defined as

$$\mathbf{u}_i \equiv \mathbf{p} + \mathbf{b}_i - \mathbf{a}_i. \tag{10}$$

Apparently, eq.(9) is quadratic in q_i, and hence, there are two IK solutions for each leg, i.e.,

$$q_i = \mathbf{e}_i^T\mathbf{u}_i \pm \sqrt{(\mathbf{e}_i^T\mathbf{u}_i)^2 - \mathbf{u}_i^T\mathbf{u}_i + l_i^2} \tag{11}$$

Once q_i known, eq.(7) can be used to compute the actuated joint angles θ_i, i.e.,

$$\theta_i = \frac{2\pi}{p_i}q_i - \gamma_i, \tag{12}$$

while γ_i depends on the EE position and is given as:

$$\gamma_i = \pm \arccos \frac{\mathbf{k}^T\mathbf{R}_i^T(\mathbf{1} - \mathbf{e}_i{\mathbf{e}_i}^T)\mathbf{u}_i}{\parallel (\mathbf{1} - \mathbf{e}_i{\mathbf{e}_i}^T)\mathbf{u}_i \parallel}, \tag{13}$$

which solve the IK problem.

2.4 Direct Kinematic Problem

The solution of the DK problem requires to find $\mathbf{p}$ that satisfy simultaneously the three kinematic loops associated to the legs of the TPM. Upon substituting eqs.(7) and (8) into (6), we obtain

$$\mathbf{p} = \mathbf{d}_i + \mathbf{s}_i(\gamma_i, \phi_i), \tag{14}$$

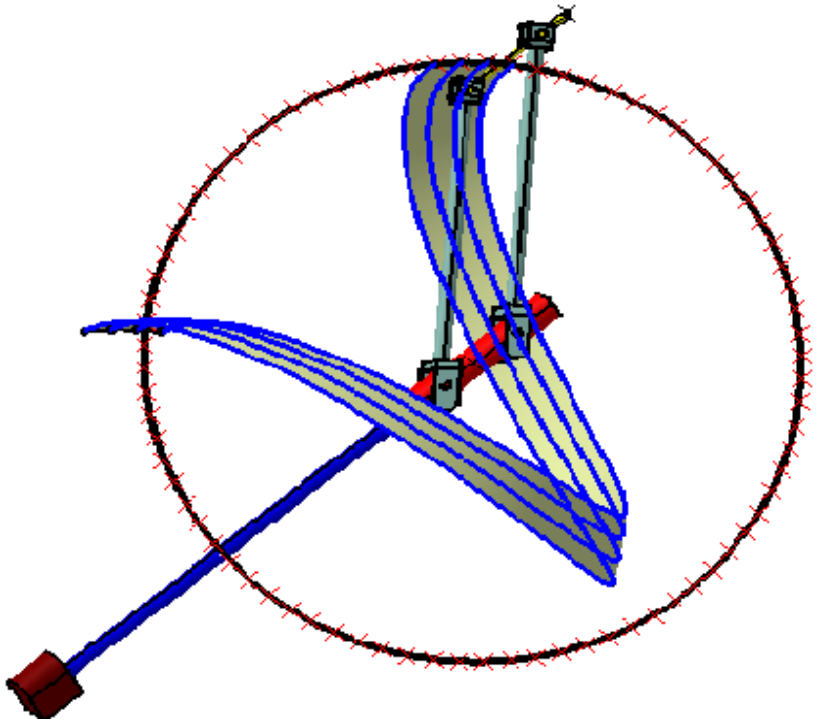

Figure 5: Possible leg end-point positions: the circle is obtained for different ϕ_i at a constant γ_i, while each helicoidal curve is obtained for different γ_i at a constant ϕ_i along the screw axis $\mathbf{e}_i$ with a pitch p_i (shown here with a very large pitch)

with

$$\mathbf{d}_i \equiv \mathbf{a}_i - \mathbf{b}_i, \tag{15}$$

$$\mathbf{s}_i(\gamma_i, \phi_i) \equiv \frac{p_i}{2\pi}(\theta_i + \gamma_i)\mathbf{e}_i + l_i \mathbf{R}_i \mathbf{R}_x(\gamma_i)\mathbf{R}_y(\phi_i)\mathbf{k}, \tag{16}$$

where $\mathbf{d}_i$ is the position vector of point D_i and $\mathbf{s}_i(\gamma_i, \phi_i)$ a *meridian-circular screw surface*[1] described by the two unknown passive rotations γ_i and ϕ_i, as shown in Fig.5. Therefore, the solution of the DK problem is the intersection points, $\{\mathbf{p}_k\}_1^K$, of three of such surfaces, i.e.,

$$\mathbf{d}_1 + \mathbf{s}_1(\gamma_1, \phi_1) = \mathbf{d}_2 + \mathbf{s}_2(\gamma_2, \phi_2), \tag{17}$$

$$\mathbf{d}_1 + \mathbf{s}_1(\gamma_1, \phi_1) = \mathbf{d}_3 + \mathbf{s}_3(\gamma_3, \phi_3), \tag{18}$$

which is a set of six nonlinear equations in six unknowns: γ_1, ϕ_1, γ_2, ϕ_2, γ_3 and ϕ_3, whose solutions $\{\gamma_1, \phi_1, \gamma_2, \phi_2, \gamma_3, \phi_3\}_1^K$ allow to compute $\{\mathbf{p}_k\}_1^K$. Whenever the pitch is zero, i.e. $p_i = 0$, the DK problem of eqs.(17) and (18) reduces to the intersection of three spheres, which has a maximum of two real solutions. Alternatively, when the pitch is different than zero, i.e. $p_i \neq 0$, the maximum number of real solutions may be much more than two as we have shown in a previous work [7]. Unfortunately, it is not possible to follow an algebraic approach

[1] Based on a personal discussion with prof. Manfred Husty from University of Loeben, Austria.

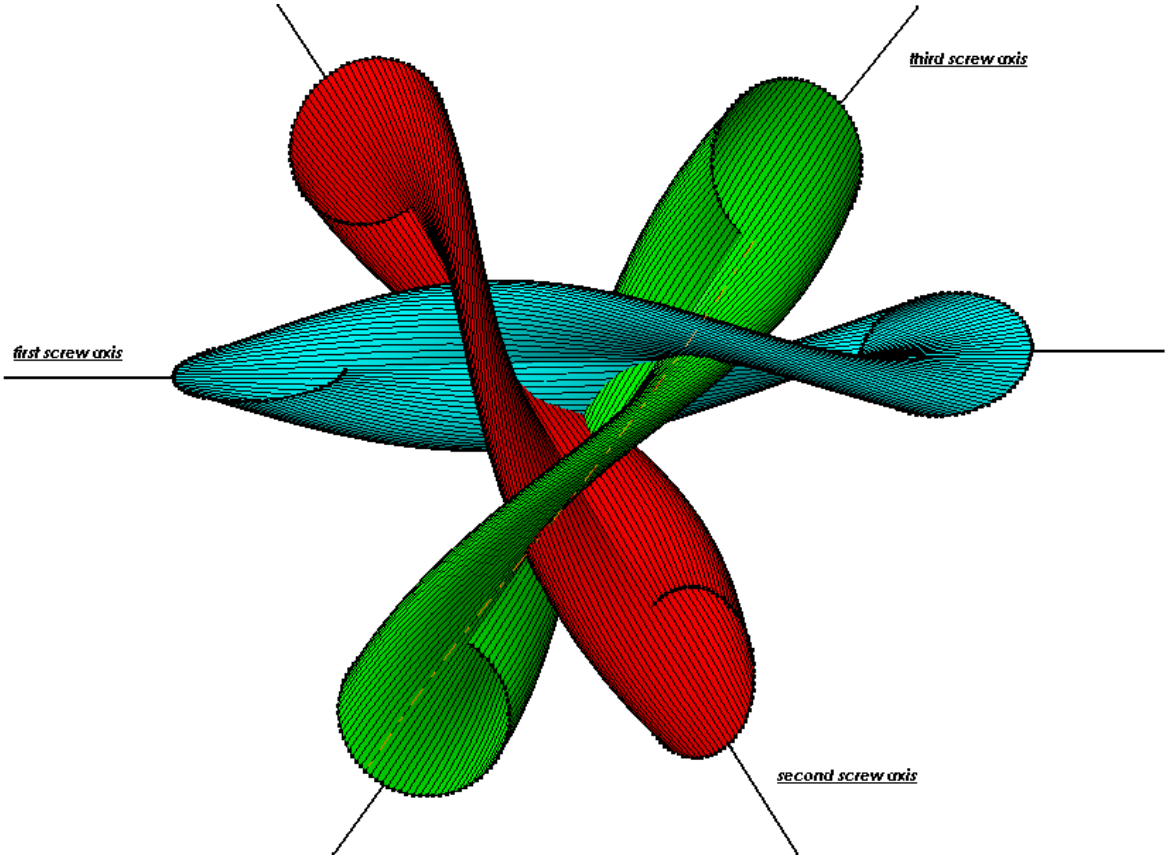

Figure 6: The three meridian-circular screw surfaces of the Y Star TPM shown here at a very large pitch

to solve this nonlinear system of eqs.(17) and (18), because the unknown ϕ_i simultaneously appear linearly and through transcendental functions. Below, we rather propose a graphical approach to solve this problem.

3 Graphical Solution Method

In this section, we present the different steps to solve the DK problem using a *Computed-Aided Design* (CAD) system, which is in our case *Catia V5R8*. The solution method is valid only for TPM, since in this case the geometry of the EE is known also in the based frame, and hence, can be subtracted from the geometry of the base as described by points D_i. The translation of each screw from A_i to D_i provides that all legs share the same attachment point to the EE, and hence, the DK problem can be solve as finding the intersection points of three shifted meridian-circular screw surfaces.

3.1 Meridian-Circular Screw Surfaces

In the *Wire-frame and Surface Design* workshop of Catia it is possible to create meridian-circular screw surfaces with the *sweep* feature by sweeping a circle along an helicoidal curve created by an *Helix* feature. Each meridian-circular screw surface is modeled in frame $\mathcal{A}_i$, and then shifted by vector $-\mathbf{b}_i$ as follows:

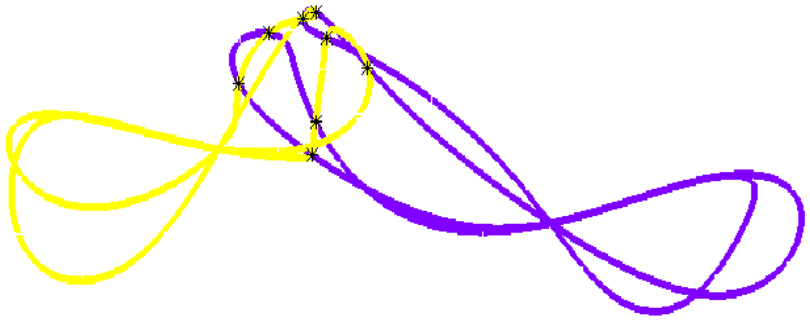

Figure 7: Intersection curves C_{12} and C_{13} with the intersection points denoted * of the two curves in 3D Cartesian space for the Y Star TPM (8 real solutions)

1. create a circle of radius l_i centered at the origin in the xy-plan of frame $\mathcal{A}_i$ is rotated around the x-axis of an angle θ_i and translated accordingly with the pitch p_i, thus defining the so-called initial circle as the one shown in Fig. 4;

2. create an helicoidal curve of pith p_i along $\mathbf{e}_i$ from an arbirairy point of the circle with the *Helix* feature such as those shown in Fig. 5

3. create a meridian-circular screw surface with the *sweep* feature by sweeping the circle as the *profile* and the helicoidal curve as the *guide curve* with the given pitch p_i;

4. finally, shift the surface by $-\mathbf{b}_i$ such as those shown in Fig. 6.

It is noteworthy that each surface represent a set of possible locations of $\mathbf{p}$ in $\mathcal{A}$ through a specific leg. Since the legs must all be simultaneously satisfied, the real solution to the DK problem are thus the intersection points of the three surfaces.

3.2 Intersection Curves

Before finding the intersection points, we first compute the intersection curve of the surfaces taken two by two with the *Intersection* feature of the *Wire-frame and Surface Design* workshop of Catia. The intersection curve of the surfaces 1 and 2, namely C_{12}, is the solution of eq.(17), while the intersection curve of the surfaces 1 and 3, namely C_{13}, is the solution of eq.(18) as shown in Fig.7.

3.3 Intersection Points

Each intersection curve, i.e. C_{12} and C_{13}, are continuous closed contours in 3D Cartesian space. The intersection points of these two contours provide all real solutions to the DK problem, which is also computed with the *Intersection* feature of Catia and shown in Fig.7.

4 Kinematic Simulation and validation

With the *Digital Mock-Up* workshop of Catia, it is possible to perform kinematic simulation of the Star TPM and also use it as a validation tool of the DK solutions. Obviously, we must be able to assemble the TPM at each of the real DK solution as we have shown in a previous work [7]. Moreover, the our implementation of this graphical solution method is generic in the sense that the geometry of the TPM is modeled in the CAD system as *parameters* through the concept of *tables*.

As a numerical example, we will compute all DK solutions of the Star TPMs with intersecting coplanar screw axes at 120^o, i.e., $v_1 = 100$, $v_2 = 100$, $v_3 = 100$, $a_2 = 0$, $a_3 = 0$, $\alpha_2 = 2\pi/3$, $\beta_3 = 0$, $\alpha_3 = -2\pi/3$, $l_1 = 100$ $l_2 = 100$, $l_3 = 100$, $p_1 = 140$, $p_2 = 140$, $p_3 = 140$; where the lengths are expressed in a nondimensional units, called u, and the actuated joints position are chosen as follows: $\theta_1 = -2rad$, $\theta_2 = -2rad$, $\theta_3 = -2rad$.

Using a CAD system, the three surfaces $\mathbf{s}_1$, $\mathbf{s}_2$ and $\mathbf{s}_3$ are generated, the intersection curves C_{12} and C_{13} are found, from which the intersection points $\{\mathbf{p}_k\}_1^K$ are computed and reported in Tables 1. Apparently, the Star TPM has in 12 DK solutions, and hence, has also 12 assembly modes as those shown in Fig.8.

Solution	x	y	z
$\mathbf{p}_1$	8.015	43.852	-65.557
$\mathbf{p}_2$	-7.176	17.638	-62.375
$\mathbf{p}_3$	-34.660	44.503	-16.562
$\mathbf{p}_4$	0.069	72.329	0.052
$\mathbf{p}_5$	31.767	44.465	-21.724
$\mathbf{p}_6$	52.833	43.735	39.654
$\mathbf{p}_7$	3.027	44.321	38.412
$\mathbf{p}_8$	57.666	17.571	42.928
$\mathbf{p}_9$	-60.722	43.603	25.988
$\mathbf{p}_{10}$	-50.407	17.578	37.451
$\mathbf{p}_{11}$	0.036	-30.082	0.085
$\mathbf{p}_{12}$	0.070	-83.667	0.085
units	u	u	u

Table 1: *The 12 real DK solutions of the Star TPM with a very large pitch at the given configuration*

5 Conclusion

We have formulated in this paper the direct kinematic problem of Star translational parallel manipulators of general geometry. The solution of this problem is equivalent to find the intersection points of three meridian-circular screw surfaces, which can have in general many intersection points. When the pitch of the screws is set to zero (in this case the topology would be described as 3-R$\underline{\text{P}}$ΠR) the DK problem reduces to the intersection points of three spheres, and hence, has in this case a maximum of two intersection points. The graphical solution method makes use of a CAD system to model the different surfaces in order to let it computes the intersection curves, and finally, the intersection points between the two curves.

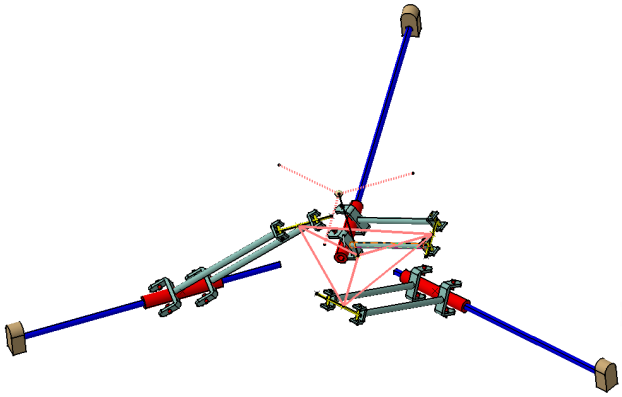

(a) assembly mode 1

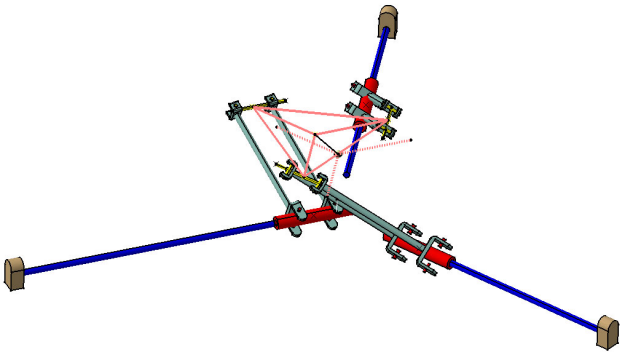

(d) assembly mode 7

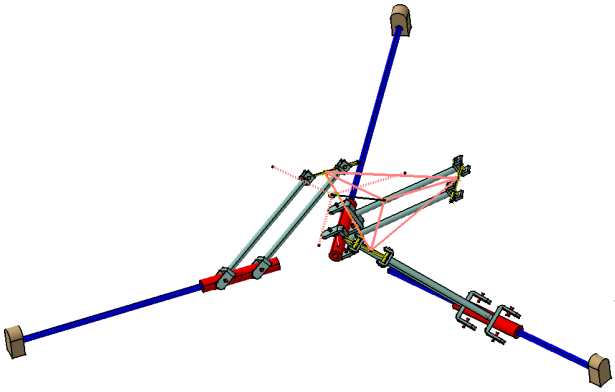

(b) assembly mode 3

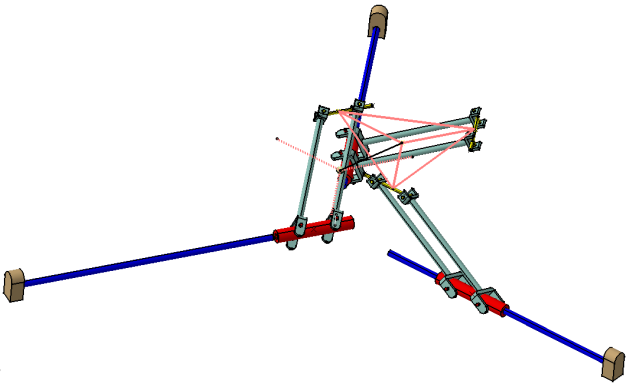

(e) assembly mode 9

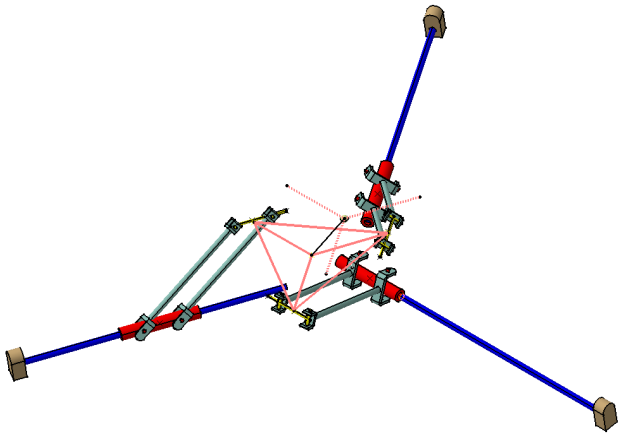

(c) assembly mode 5

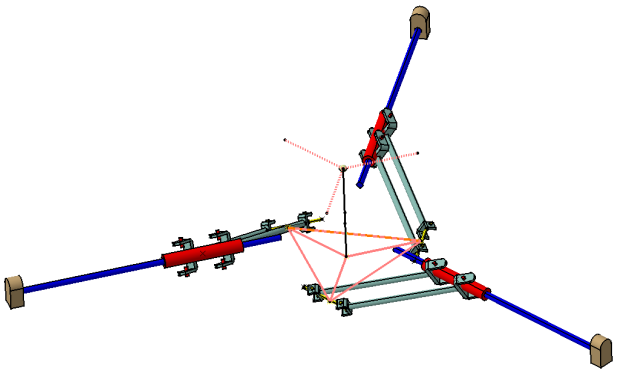

(f) assembly mode 11

Figure 8: Assembly mode 1, 3, 5, 7, 9 and 11 of the Star TPM

Acknowledgments

The authors acknowledge the financial support of NSERC (National Sciences and Engineering Research Council of Canada) under grants RGPIN-203618 and RGPIN-150270, and FCAR (Fond concerte d'aide a la Recherche of Quebec) under grants NC-66861 and ER-3618.

References

[1] Hervé, J.M., "Dispositif pour le déplacement en translation spaciale d'un élément dans l'espace, en particulier pour robot mécanique", *French Patent No. 9100286*, January 1991, *European Patent No. 91403521.7*, December 1991.

[2] Baron, L. and Angeles, J., "The Direct Kinematics of Parallel Manipulators Under Joint-Sensor Redundancy", *IEEE Trans. on Robotics and Automation*, Vol. 16, No. 1, pp. 12–19, January 2000.

[3] Hervé, J.M. and Sparacino, "Star, a new concept in robotics,", *Advances in Robot Kinematics*, pp. 176–183, Ferrare, Italy, Sept. 7-9, 1991.

[4] Baron, L., "Workspace-Based Design of Parallel Manipulators of Star Topology With a Genetic Algorithm", *ASME Design Automation Conference*, Pittsburgh, USA, Sept. 9–12, 2001.

[5] Baron, L. and Bernier, G.,"The design of parallel Manipulators of Star Topology Under Isotropic Constraint", *ASME Design Automation Conference*, Pittsburgh, USA, Sept. 9–12, 2001.

[6] Angeles, J., 2002, "The Qualitative Synthesis of Parallel Manipulators", *Proc. of the Workshop on Fundamental Issues and Future Research Directions for Parallel Mechanisms and Manipulators*, Quebec, pp. 160–169.

[7] Sayd, M., Baron, L. and Mascle, C., "The Star Parallel Manipulators Can Have More Than Two Assembly Modes", *IEEE Int. Conf. on Control and Automation*, Montreal, Canada, June 9–12, 2003.